Published in final edited form as:
J Comp Neurol. 2008 December 1; 511(4): 543–556. doi:10.1002/cne.21862.

Visualizing Mechanosensory Endings of TrkC-Expressing Neurons Using HS3ST-2-hPLAP Mice

Hiroshi Hasegawa[#] and **Fan Wang**[*]
Department of Cell Biology, Duke University Medical Center, Durham, NC 27710, USA

Abstract

Somatosensory neurons are classified into three main types according to their modalities: nociceptive, thermal and mechanosensory. Within each modality group, neurons can be further divided into morphologically and functionally distinct subclasses. Here we show that *Heparan sulfate D-glucosaminyl 3-O-sulfotransferase 2* (*HS3ST-2*) is a marker for specific subsets of TrkC-expressing cutaneous low threshold mechanosensory and proprioceptive mechanosensory neurons. Two-color *in situ* analysis revealed almost all *HS3ST-2* signals co-localized with *TrkC*, but not with *TrkA* or *TrkB* mRNA. To visualize the morphological subtypes of *HS3ST-2*/TrkC-expressing neurons, we generated a HS3ST-2-hPLAP knock-in mouse line, in which *HS3ST-2*-expressing neurons and their projections are labeled by human placental alkaline phosphatase (hPLAP). AP-staining in these mice demonstrated that sensory endings of muscle spindles and Golgi tendon organs as well as the cutaneous mechanosensory Merkel and longitudinal lanceolate endings in the whiskers are strongly positive for hPLAP activity. In contrast, no nociceptive endings are labeled. In the glabrous and hairy skin, rare Merkel endings and transverse lanceolate endings are weakly stained. During development, each type of nerve endings forms at different time point. Muscle innervations differentiate first, followed by formation of cutaneous sensory endings. Our results revealed the subtype identities of TrkC-positive mechanosensory neurons and demonstrated the usefulness of *HS3ST-2* as a genetic marker for these subclasses of neurons.

Keywords

sensory ganglia; genetic labeling; mechanosensory nerve endings; development; hPLAP; HS3ST-2

INTRODUCTION

Somatosensory neurons, located in trigeminal ganglia (TG) or dorsal root ganglia (DRG), sense diverse modalities of sensory signals from both the external environment and from the body itself. These sensations include pain, temperature, touch and body posture. In order to detect these complex stimuli accurately, somatosensory neurons differentiate into many subtypes, each of which is believed to transduce specific kinds of sensory information. Previous studies have tried to identify molecular markers whose expression is specifically associated with neurons of distinct sensory modalities. The receptors for neurotrophic factors (Trks) are the best characterized markers as their expression patterns are closely, but not exactly, related to specific modalities. It has been shown that, in DRG, TrkA and cRet

[*]Correspondence should be addressed to: Fan Wang, Department of Cell Biology, Duke University Medical Center, Box 3709, Durham, NC 27710. Tel: 919-684-3682, Fax: 919-684-8090, E-mail: f.wang@cellbio.duke.edu.
[#]Present address, Graduate School of Comprehensive Human Sciences, University of Tsukuba, Tsukuba, Japan

We ask Dr. Gert Holstege to be the review editor.

are mainly expressed by the nociceptive and thermosensory neurons that sense pain and temperature (e.g. Chen et al., 2006). TrkB is expressed by a subpopulation of cutaneous low threshold mechanosensory neurons (Barbacid, 1994; Carroll et al., 1998). TrkC is found in the commonly called proprioceptive neurons (which are in fact mechanosensory neurons that are interceptors) innervating the skeletal muscles, although some types of cutaneous mechanoreceptors also express TrkC and their survival requires TrkC signaling (Ernfors et al., 1994; Klein, 1994). The association of Trk receptors with sensory modalities is more complicated in trigeminal ganglia (TG), as it was shown that TrkA, TrkB or TrkC are all required for the proper development and survival of the entire sets of cutaneous mechanosensory neurons (Fundin et al., 1997; Cronk et al., 2002). Thus, the Trk receptors are not strictly correlated with the modality specificity in somatosensory neurons (Rice et al., 1998; Huang and Reichardt, 2003; Funfschilling et al., 2004). Within the nociceptive/thermosensory population of neurons, expression of other molecular markers such as CGRP, IB4+, *TrpV1*, *TrpM8*, *TrpA1*, and various *Mrg* genes further divide nociceptive neurons into different subtypes (Caterina et al., 1997; Molliver et al., 1997; Snider and McMahon, 1998; Dong et al., 2001; McKemy et al., 2002; Peier et al., 2002; Story et al., 2003; Zylka et al., 2003). However, much less is known about markers for subtypes of mechanosensory neurons.

In rodents, the whiskers are the primary tactile organs. Each whisker is innervated by at least seven different types of morphologically-distinct mechanosensory nerve endings originating from the trigeminal ganglia. They are classified as: (a) superficial ridge Merkel endings; (b) transverse lanceolate endings; (c) longitudinal lanceolate endings; (d) outer hair root Merkel endings; (e) club-like ringwulst endings; (f) reticular endings; and (g) spiny (Ruffini) endings (Fundin et al., 1997; Ebara et al., 2002). It is thought that the combinatorial activities of these seven types of input encode the nature of tactile stimuli. Previous studies have demonstrated that deficiency in any of the neurotrophins or any of the neurotrophic receptors (TrkA/B/C and p75) caused reduction/absence of certain subclasses of whisker touch neurons (Fundin et al., 1997; Cronk et al., 2002). However, since neurotrophins and their receptors are expressed not only by sensory neurons but also by cells in whisker follicles, some of the neuronal phenotypes may be secondary to the defects of whisker follicle development. It remains unclear which subclass of touch-sensing trigeminal neurons express which receptors and which signaling pathway is primarily responsible for a specific type of nerve endings.

Heparan sulfate D-glucosaminyl 3-O-sulfotransferases (3OSTs, HS3STs) are key components in generating specific heparin sulfate sequences that regulate various important biological activities of heparan sulfate proteoglycans (Lee and Chien, 2004; Lin, 2004). HS3STs are composed of six subtypes, which are known to have different substrate specificities (Liu et al., 1999; Shworak et al., 1999; Xia et al., 2002; Chen et al., 2003; Xu et al., 2005). Most of the HS3STs are widely expressed throughout the body, including the nervous system (Shworak et al., 1999; Xu et al., 2005; Yabe et al., 2005; Cadwallader and Yost, 2006; Lawrence et al., 2007).

In this paper, we show that *HS3ST subtype 2* (*HS3ST-2*) is expressed by a subset of cells in the developing mouse trigeminal ganglia (TG). We found that, from late embryonic stages till adulthood, most *HS3ST-2* is primarily expressed in TrkC-positive neurons and in very few cRet-positive neurons. *HS3ST-2* is not expressed by TrkA- and TrkB-positive trigeminal neurons or by hair follicle cells. Thus, we can use *HS3ST-2* to definitively label TrkC-positive neurons. We generated HS3ST-2-hPLAP mice, in which the start ATG codon of *HS3ST-2* gene was replaced by the *human placental alkaline phosphatase* (*hPLAP*). The hPLAP protein is a heat-insensitive and membrane-bound alkaline phosphatase that is transported to the surface of axons (Leighton et al., 2001; Shah et al., 2004; Zylka et al.,

2005). These mice allowed us to visualize specific sensory endings formed by TrkC/*HS3ST-2*-expressing neurons in the TG and DRG. We found that TrkC-positive TG neurons give rise to mostly Merkel endings and longitudinal lanceolate endings in the whiskers, and that most TrkC-positive DRG neurons form muscle spindle and Golgi tendons endings in skeletal muscles.

MATERIALS AND METHODS

Generation of HS3ST-2-hPLAP mutant mice

The *HS3ST-2* genomic fragment was obtained from BAC clone RP23-400L7. We constructed the targeting vector by inserting the *hPLAP-ACN* cassette (Zylka et al., 2005) into the translation start ATG of the *HS3ST-2* gene. Targeted ES cells were generated and confirmed by Southern blotting.

To detect the HS3ST-2-hPLAP mutant allele by PCR, PCR primers were designed as follows: *3OST2/04*, 5′-AGATGCTGGCAATGCAGCCACC-3′; *3OST2/05*, 5′-GCTGTAACACAGGTAAGTGC-3′; *hPLAP/06*, 5′-AGAACCCGGACTTCTGGAACC-3′; *hPLAP/07*, 5′-TTCATCACGGAGATGACCTC-3′. The wild type allele produces a ~350 bp fragment with *3OST2/04* and *3OST2/05* primers, whereas the mutant allele is detected by a ~700 bp fragment with *hPLAP/06* and *hPLAP/07* primers. All animal experiments were conducted according to protocols approved by The Duke University Institutional Animal Care and Use Committee.

In situ hybridization

The mouse cDNA sequence for the *HS3ST-2* gene was amplified from mouse trigeminal ganglia cDNAs using primers containing the T7 promoter sequence. The sequences of the primers were as follows: *3OST2/F*, 5′-GCGAATTAACCCTCACTAAAGGGAGACTTGTCTCTTCCGCAAGGTTTG-3′; *3OST2B*, 5′-GCGTAATACGACTCACTATAGGGAGATTATGTGCTTTTGTCCGCAGG-3′. *In vitro* transcription was then performed from the PCR-amplified template using T7 RNA polymerase (Roche) with Digoxigenin-UTP (Roche) for synthesis of the antisense probe for *HS3ST-2* mRNA. *In situ* hybridization was performed according to standard methods previously described (Hodge et al., 2007).

The two color-*in situ* hybridization was performed as described previously (Dong et al., 2001; Luo et al., 2007). DIG-labeled *HS3ST-2* probe is paired with FITC-labeled *TrkA*, *TrkB*, *TrkC* or *cRet* probe for co-localization studies. For the generation of probes, the following sequences were used as primers: *TrkA/F*, 5′-TTCTGCCCTCCTTCTTGTGCTC-3′; *TrkA/B*, 5′-GCGTAATACGACTCACTATAGGGATCGCTCTCGGTGCTGAACTTG-3′; *TrkB/F*, 5′-ATTTCCGCCACCTTGACTTGTC-3′; *TrkB/B*, 5′-GCGTAATACGACTCACTATAGGGTTTTGTTCGTAGTATCCCCAATGTC-3′;*TrkC/F*, 5′-TTTGCCTGATGTGGACTGGATAG-3′; *TrkC/B*, 5′-GCGTAATACGACTCACTATAGGGTTCAACACGATGTCTCTCCTC-3′; *cRet/F*, 5′-ACCAGGTTCCTGTGGACTCTTTC-3′; *cRet/B*, 5′-GCGTAATACGACTCACTATAGGGAGATCTGAGAGCCCATCGTCATACAG-3′.

Antibody Characterization

Rabbit anti-PGP9.5 polyclonal antibody (RA95101, UltraClone, UK, 1:1000) was raised against purified human PGP9.5 protein (27kD) from pathogen-free human brain, and it cross-reacts with PGP9.5 in all mammalian species so far tested (manufacturer's technical

information). It was discovered that this anti-PGP9.5 antibody stains neuronal cell bodies and axons in the central and peripheral nervous system (Wilson et al., 1988 and manufacture's technical information). Since then, it has been extensively used simply as a marker for neurons and nerve fibers by numerous labs showed in many publications (e.g. Rice et al., 1998; Funfschilling et al., 2004; Zylka et al., 2005), and we have observed similar staining patterns of peripheral nerve fibers as others have previously described (Figure 6). Rabbit anti-neurofilament 200 kD polyclonal antibody (AB1982, Chemicon/Millipore, Temecula, CA; 1:200) is raised against highly purified bovine 200kDneurofilament protein. By immunoblotting, it stains a band at 200 kD and bands around 170–180 kD (manufacturer's technical information). This antibody has been widely used to stain large-diameter sensory neurons (e.g. Cronk et al., 2002; Funfschilling et al., 2004) and we have observed similar staining patterns (Figure 7). Rabbit anti-calcitonin gene related peptide (CGRP) polyclonal antibody (AB5920, Chemicon/Millipore; 1:3000) is raised against synthetic rat CGRP neuropeptide. Using this antiserum, we observed the anti-CGRP-immunoreactive nerve endings similar as previously described by many others (Figure 7, and see Kramer et al., 2006; Torsney et al., 2006; Yoshikawa et al., 2007; Chao et al., 2008).

Immunofluorescence

Adult mice were anesthetized and perfused with 4% paraformaldehyde (PFA)/phosphate buffered saline (PBS) (pH=7.4) through the cardiac tissue. Dissected tissues were postfixed in 4%PFA/PBS on ice for 3 hours. Embryos were dissected out from timely-pregnant female and fixed in 4% PFA/PBS on ice for 3 hours. They were then protected in 30% sucrose/PBS at 4°C overnight. Tissue sections were collected with a cryostat at 12 μm thickness. The sections were fixed in 4% PFA/PBS at room temperature for 10 minutes and washed in PBS for 3 minutes three times. Then, they were blocked in H-PHT buffer (5% normal goat serum, 0.1% Triton X-100 in PBS) for 2 hours at room temperature (r.t.) and incubated with primary antibodies at 4°C overnight. After washing with H-PHT five times, the signals were visualized by incubating with Alexa^{488}-labeled goat anti-rabbit IgG (H+L) (A11008, Molecular Probes of Invitrogen, Eugene, OR; 1:400) for 2 hours at r.t. The images were acquired with HR Axiocam (Zeiss) and OpenLab software (Improvision). Brightness and contrast were increased slightly for all images using Adobe PhotoShop software (Adobe).

Alkaline phosphatase staining and co-staining with anti-PGP9.5 antibodies

AP-staining was performed as described (Leighton et al., 2001). Tissue sections were collected with a cryostat at 12–30 μm thickness. The sections were post-fixed with 4% PFA/PBS at room temperature for 1 hour, followed by incubation at 65°C for 4 hours in PBS. For the detection of alkaline phosphatase activity, the sections were rinsed with wash buffer (0.1 M Tris-HCl (pH 7.5), 0.1 M NaCl) and then incubated in developing buffer (1:200 NBT/BCIP stock solution (Roche), 0.1 M Tris-HCl (pH 9.5), 0.1 M NaCl, 5 mM $MgCl_2$). The reaction was stopped by washing in PBS three times.

For immunofluorescent staining combined with chromogenic AP-staining, AP-staining was carried out first. Afterwards, sections were then with rabbit anti-PGP9.5 polyclonal antibody at 4°C overnight and detected with Alexa^{488}-labeled goat anti-rabbit IgG (H+L) (1:400).

RESULTS

Expression pattern of *HS3ST-2* mRNA in mouse sensory neurons

Using *in situ* hybridization analysis, *HS3ST-2*was found to be expressed in the mouse craniofacial and somatosensory ganglia but not in cutaneous tissues (Fig 1 and data not shown). In neonatal TG, its signal was observed in a subset of neurons with differential

expression levels. A subset of sensory neurons is strongly positive for *HS3ST-2* (Fig 1A, inset, arrow), whereas another subset expresses the gene weakly (Fig 1A, inset, arrowheads). Most of the *HS3ST-2*-positive neurons were found in the ophthalmic and maxillary division of the TG; while very few neurons in the mandibular division were positive (data not shown). *HS3ST-2* signal was also detected in a few neurons in the facial (VII), the glossopharyngeal (IX), and the vagus (X) ganglia, in which there appeared to be only low expressing cells (Fig 1B and E). Interestingly, *HS3ST-2* is strongly expressed by all neurons in the vestibular (a part of VIII) ganglia, whereas no signal was observed in the cochlear (the other part of VIII) ganglia (Fig 1C and D).

We next examined the expression pattern of *HS3ST-2* in sensory neurons during embryonic development. At E10.5, *HS3ST-2* has not yet expressed in the TG (data not shown). The signal was first detected at E11.5 (data not shown), and the intensity gradually increased from E12.5 to E14.5 (Fig 1F and G). From E11.5 to E14.5, *HS3ST-2* is expressed at higher levels in the ophthalmic and maxillary divisions and lower levels in the mandibular division, but the overall level is low (Fig 1F and G). Although almost all cells in the ophthalmic and maxillary divisions express *HS3ST-2* at E12.5, strong punctuate signals start to appear at E14.5 (Fig 1G, arrows), indicating a subset of neurons begin to strongly express the *HS3ST-2* mRNA at this stage. At E16.5, high *HS3ST-2* expression is restricted to only a small population of cells (Fig 1H). This pattern continues into the adult stage (Fig 1A and data not shown). Similarly, *HS3ST-2* is expressed in most of the cells in the early embryonic facial (VII) ganglia (Fig 1F and G, data not shown), whereas only a subset of VII ganglia neurons is positive at later stages (Fig 1B).

In contrast to the TG, the *HS3ST-2* was not detected in the DRG at E11.5 and E12.5 (Fig 1I and data not shown). The strong signal in a few neurons began to be detected at E14.5 (Fig 1J). These results suggest that the expression of *HS3ST-2* is differently regulated in the TG and the DRG at the earlier stages, although its expression is similarly restricted to a subset of neurons in the late embryonic and postnatal stages.

Examining the co-localization of the *HS3ST-2* with neurotrophic factor receptors

In order to characterize the identity of *HS3ST-2*-positive neurons, two-color *in situ* hybridization analyses on DRG and TG sections were performed using RNA probes for *TrkA*, *TrkB*, *TrkC* and *cRet*. It is known that in the DRG, most of *TrkA*- or *cRet*-positive neurons are small diameter nociceptive/thermosensory neurons, whereas *TrkB* and *TrkC* mainly label a subset of medium to large diameter mechanosensory neurons, respectively (Fig 2A, E, I and M) (Snider, 1994; Molliver et al., 1995; Priestley et al., 2002). Almost all *HS3ST-2* signals were co-localized with *TrkC* signals and very few *HS3ST-2* were seen in *cRet*-positive cells, whereas no co-localization of *HS3ST-2* with *TrkA* and *TrkB* expressing neurons was observed (Fig 2A–P). These results suggest that the majority (over 95%) of the *HS3ST-2*-positive cells are *TrkC*-expressing neurons in the DRG, and that the rest are in a few *cRet*-positive neurons. Conversely, 89.7% ± 0.9% of *TrkC*-positive neurons express *HS3ST-2*, i.e. *HS3ST-2* is expressed in most but not all TrkC neurons (TrkC-positive neurons that do not express *HS3ST-2* are indicated by arrowhead in Fig 2I–L).

In neonatal trigeminal ganglia (TG), similar to the results from DRG, 93.1% ± 1.7% of *HS3ST-2*-positive neurons express *TrkC* and do not express *TrkA* or *TrkB*; and very few *HS3ST-2*-positive cells co-localize with *cRet* (Fig 3). There are high- and low-*HS3ST-2* expressing neurons within the *TrkC*-positive population of TG neurons (Fig 3I–L), while all of the rare *HS3ST-2*- and *cRet*-double positive neurons express *HS3ST-2* at a low level (Fig 3M–P). One fourth of TrkC-positive TG neurons in the ophthalmic and maxillary region lack *HS3ST-2*. Thus, *TrkC*-positive TG neurons can be classified into three subtypes according to the expression level of *HS3ST-2*: 36.2% ± 3.3% high-, 39.2% ± 2.1% low-, and

24.5% ± 2.9% no expression. Taken altogether, these results indicate that *HS3ST-2* is primarily expressed in *TrkC*-positive TG and DRG neurons, with the exception of very few *cRet*-positive cells.

Generation of *HS3ST-2*-hPLAP mice

Since TrkC is expressed in cutaneous tissues such as hair and epidermis (Botchkarev et al., 1998; Adly et al., 2005), it is difficult to clearly visualize the morphology of TrkC-positive sensory endings within these tissues using either anti-TrkC immunohistochemistry or other genetic labeling methods. In contrast, *HS3ST-2* is not expressed in either skin or muscle, thereby can be used to determine the specific sensory subtype of the TrkC-expressing neurons. To achieve this genetically, we constructed a targeting vector in which the start ATG codon of the *HS3ST-2* gene was replaced by the gene encoding hPLAP (Fig 4A), which enables us to trace all axons of the *HS3ST-2*-positive neurons (Leighton et al., 2001; Shah et al., 2004; Zylka et al., 2005). Knock-in mice were generated and their genotype was confirmed by both Southern blotting (Fig 4B) and genomic PCR (Fig 4C). Both heterozygous and homozygous HS3ST-2-hPLAP mice showed no abnormality in their appearance, behavior or fertility and lived healthy up to at least one year (data not shown).

To confirm the expression of hPLAP protein and its activity, we performed the AP-staining of the TG and DRG sections from heterozygous HS3ST-2-hPLAP mice. The intense hPLAP activity was detected in a subset of cells in both adult TG (Fig 5G) and DRG (Fig 5H). Consistent with the *in situ* hybridization data shown above, some of the hPLAP-positive cells are densely stained by AP-activity, whereas others are stained lightly; this again suggests the existence of two different expression levels of *HS3ST-2* in both TG and DRG neurons in adult.

During development, the hPLAP expression was found as early as E12.5 in TG, when the expression level was high in the rostral region (ophthalmic and maxillary divisions) and low in the caudal region (mandibular division) (Fig 5A and B). Some cells began to strongly express hPLAP at E14.5, and other cells lost the hPLAP expression with age (Fig 5C and D). Three different expression levels, high, low and no expression, became apparent after E16.5 (Fig 5D–G). These results suggest that hPLAP-expression completely recapitulates the endogenous expression pattern of *HS3ST-2*.

Visualization of peripheral innervations from *HS3ST-2*-expressing TG neurons in the whisker pads

The HS3ST-2-hPLAP mice allow us to use the AP-staining to visualize all axons and nerve endings of the *HS3ST-2*-expressing (and hence most of the TrkC-positive) neurons. Whiskers are the most important tactile-sensory organs in rodents. The follicle sinus complex (FSC) within each whisker is innervated by several morphologically different types of trigeminal mechanosensory nerve endings (Rice et al., 1993; Fundin et al., 1994; Davis et al., 1997; Rice et al., 1997; Ebara et al., 2002), whereas the surface skin, in contrast, is innervated by a set of morphologically distinct and primarily nociceptive/thermosensory axons (Rice et al., 1998).

We first examined the projection of *HS3ST-2*-positive axons in the mystacial (whisker) pads during development. At E12.5, when the whisker buds begin to emerge and *HS3ST-2* was detected mainly in the ophthalmic and maxillary division, hPLAP-positive axons were already found in the presumptive whisker follicles (Fig 5I). These axons form axon bundles underneath the whisker buds and some of the bundles around the presumptive whisker follicle form a “basket” structure. At E14.5, when the whisker follicles are clearly visible, the axons project alongside the whisker follicles to the level of the ring sinus (Fig 5J). These

axons have not yet formed morphologically-differentiated nerve endings. At E16.5, the HS3ST-2-hPLAP positive axons began to form the Merkel endings at the ring sinus level (Fig 5K). Interestingly, at both stages (E14.5 and E16.5), the axons at the dorsal side of the developing FSC were more intensely stained by the AP-activity than the axons at the ventral side (arrows in Fig 5J and K), while anti-PGP9.5 staining showed equal intensity at both the dorsal and the ventral side of the whisker follicles (data not shown). Considering that the *HS3ST-2* begins to be strongly expressed in a subset of neurons at E14.5, the neurons innervating the dorsal side of the developing FSC may be expressing a high-level of *HS3ST-2* first. The axons at the ventral side were equally stained at P0 (Fig 5L), suggesting the neurons innervating at the ventral side become positive for *HS3ST-2* at the later stages.

In order to examine which types of nerve endings originate from the *HS3ST-2*-expressing neurons, we analyzed the hPLAP-positive axons and nerve endings in the adult mystacial pads of heterozygous HS3ST-2-hPLAP mice (Fig 6). Some of the sections were first stained by the hPLAP activity, followed by the immunostaining with anti-PGP9.5 antibody (Fig 6C–J). Note that the purple reaction product of AP-staining significantly masks the fluorescent signal of anti-PGP9.5 staining, making it somewhat difficult to see the co-localization of both signals. Using this method, we found that the longitudinal lanceolate endings and the Merkel endings located in the outer root sheath, which are derived from the deep vibrissal nerves (DVN), are two most prominent endings stained for AP-activity (and thus expressing *HS3ST-2*/TrkC) (Fig 6A and B). The longitudinal lanceolate endings are also positive for NF200 (Fig 7E and F), but very weakly positive for CGRP (Funfschilling et al., 2004) (Fig 7I and J). Merkel endings are positively stained with anti-NF200 but are negatively stained for anti-CGRP (Fig 7E and I), whereas Merkel cells are CGRP-positive (Fig 7I, J and K). The DVN nerves also supply the reticular endings, the club-like endings and the spiny (Ruffini) endings. We found that the reticular and club-like endings completely lack hPLAP staining (Fig 6G–J), indicating they do not express *HS3ST-2* at all. Weak hPLAP activity was found in a small number of the spiny endings (Fig 6E and F, arrowheads), which are NF200-positive and CGRP-negative (Fig 7D, H and L). The superficial vibrissal nerves (SVN) form two types of nerve endings: the Merkel endings in the rete ridge collar and the transverse lanceolate endings in the inner conical body of the FSC. The SVN-derived NF200-positive Merkel endings were strongly positive for the hPLAP activity (Fig 7A and E). Thus, all Merkel endings (superficial or deep in the FSC) express *HS3ST-2*/TrkC. In the inner conical body, a very small subset of the circumferential endings was also stained albeit very weakly for AP-activity (Fig 6C and D, arrows). There are three distinct types of circumferential endings in the inner conical body, including (1) peptidergic, NF200-negative and CGRP-positive C fibers, (2) non-peptidergic, NF200- and CGRP-negative C fibers, and (3) NF200-positive and CGRP-negative Aβ fibers, called transverse lanceolate endings (Funfschilling et al., 2004). Our analysis could not clearly distinguish which types of nerve endings are HS3ST-2-positive, due to technical limitations. However, considering that the size of the endings is relatively large and that *HS3ST-2* is not expressed in TrkA-positive neurons (Fig 3), these results suggest that these hPLAP-weak positive nerve endings are a small subset of Aβ fibers with the transverse lanceolate endings.

Taken together, our results argue strongly that the Merkel endings and the longitudinal lanceolate endings originate from the TrkC-positive neurons that strongly express *HS3ST-2*. The *HS3ST-2*-weakly-positive trigeminal neurons form a type of circumferential circular endings (probably transverse lanceolate endings) and the spiny endings; these could be either TrkC- or cRet-expressing neurons. All reticular endings and club-like endings, originate from *HS3ST-2*-negative (probably TrkC-negative) neurons. The trigeminal nociceptive axons distributed in the surface of skin were completely negative for hPLAP activity, indicating that *HS3ST-2* is not expressed in the nociceptive neurons and that it is a specific marker for subtypes of cutaneous (low-threshold) mechanosensory TG neurons.

Visualization of central and peripheral innervations from *HS3ST-2*-expressing DRG neurons

We next examined the expression of hPLAP in the developing DRG and spinal cord. Consistent with the *in situ* hybridization data, the hPLAP activity was not detected in E12.5 DRG (Fig 8A). The hPLAP signal was found in motor columns and in the axons of the ventral spinal tract, including the spinocerebellar and vestibulospinal tracts (Fig 8A, arrow and arrowhead). The ventral motor roots were weakly positive for hPLAP activity, suggesting that some of the motor neurons express low-level *HS3ST-2* at this stage (Fig 8A, open arrow). The strong expression of hPLAP in the DRG can be seen at E14.5 and is found only in a subset of the cells (Fig 8B). In the spinal cord, the Ia fibers innervating the motor columns were clearly visualized by AP-staining (Fig 8B, arrows) and some of the axons innervating layer III/IV, which are cutaneous mechanosensory axons, are also weakly positive for hPLAP activity (Fig 8B, arrowheads). In contrast, in layer I/II where the nociceptive/thermosensory afferents from DRG neurons innervate, AP-activity was absent. The central projection pattern is consistent with our *in situ* studies showing that *HS3ST-2* labels the majority of TrkC-expressing (proprioceptive/mechanosensory) neurons and a very small population of cRet-expressing cells. These patterns of AP-staining in the DRG and their central afferents are essentially the same at E16.5 and P0, and persist into the adult (Fig 8B–D, data not shown).

To visualize the peripheral sensory endings formed by *HS3ST-2*-positive DRG neurons, we stained the sections containing the glabrous skin or skeletal muscles from heterozygous mice (Fig 9). The glabrous skin of the footpad is largely devoid of AP-activity (Fig 9A). Upon high-magnification examination, we found a very small number of Merkel endings expressing HS3ST-2-hPLAP with very weak signal intensity (Fig 9B-C). In contrast, strong hPLAP signal is detected in the skeletal muscles, in which sensory endings innervating both muscle spindles and Golgi tendon organs are clearly stained (Fig 8G and 9D). In the hairy skin, the transverse lanceolate endings surrounding guard hairs are also weakly positive for the hPLAP activity, whereas no signal was detected on the longitudinal lanceolate endings or Merkel endings (Fig 9E and F). No nociceptive endings projecting to the surface of the skin are hPLAP-positive. These results further confirm that TrkC-positive skeletal muscle innervating neurons strongly express *HS3ST-2* mRNA, and suggest that perhaps a small percentage of TrkC- and cRet-positive neurons that express low level *HS3ST-2* form a subset of Merkel endings in glabrous skin and the transverse lanceolate endings around guard hairs.

Development of the peripheral nerve endings in skeletal muscles

We next visualized the developmental process of the sensory ending formation in the skeletal muscles in embryos. The first muscle fibers are known to appear at E11.5–12.5 (Buckingham et al., 2003). In the skeletal muscles of E14.5 heterozygous HS3ST-2-hPLAP mice, the sensory axons, which are strongly positive for the AP-activity, have reached their target area and appear as clusters of nerve endings (Fig 8E and F). By E16.5, both the muscle spindles and Golgi tendon organs innervations are further differentiated, but are still immature (data not shown). The differentiated endings were found at P0 (Fig 8G). Thus, the differentiation of muscle-innervating nerve endings begins earlier than the formation of cutaneous mechanosensory nerve endings in the glabrous skin of the footpads and in hairy skin of back, which are formed during the postnatal stages (Peters et al., 2002; Hasegawa et al., 2007). As we mentioned above, the motor columns and the ventral motor root were weakly positive for the AP-activity at E12.5 in HST3ST-2-hPLAP mice (Fig 8A). However, we did not detect any hPLAP-positive neuromuscular junctions in the P0 and adult skeletal muscles (data not shown), indicating the motor neurons probably lose the expression of *HS3ST-2* at late embryonic stages.

DISCUSSION

Here we studied the expression pattern of *HS3ST-2* mRNA in the developing embryos and found this gene is expressed in the majority of TrkC-positive as well as in very rare cRet-positive primary somatosensory neurons. We took advantage of this genetic locus and generated a mouse model in which the axonal projections of *HS3ST-2*-positive TG and DRG neurons are labeled by a neuronal tracer, hPLAP. In these mice, the development of proprioceptive mechanosensory and subclasses of cutaneous low threshold mechanosensory nerve endings can be clearly visualized. This study demonstrated that the cutaneous mechanosensory neurons that give rise to Merkel endings and longitudinal lanceolate endings are TrkC-positive neurons.

Developmental expression of *HS3ST-2*

In the early stages (E11.5 and E12.5), *HS3ST-2* is weakly expressed in all cells in the ophthalmic and maxillary but not in the mandibular division of the TG (Fig 1). Around E14.5, TrkC-positive neurons begin to strongly express *HS3ST-2* and other neurons lose their expression (Fig 1). Such a dynamic change of *HS3ST-2* expression levels may indicate that unknown intrinsic or extrinsic factors restrict and upregulate*HS3ST-2* expression at this stage. Our data revealed that the expression level of the *HS3ST-2* in the DRG is correlated with the final target of the axons; neurons innervating skeletal muscles express high level of *HS3ST-2*, whereas neurons innervating glabrous and hairy skin express lower. Thus, target-derived signals might be critical for determining neuronal gene expression and differentiation. In the trigeminal ganglia, significantly more *HS3ST-2*-positive neurons are seen in the maxillary division. This correlates well with the fact that large whiskers are located on the maxillary region of the face and are innervated by *HS3ST-2*-positive neurons. Perhaps factors expressed in whisker follicles can retrogradely regulate *HS3ST-2* expression.

Most of the *HS3ST-2* signals are found in TrkC-positive neurons at late embryonic stages. Although TrkC is expressed only in a subset of neurons in the adult TG, Funfschilling et al. (2004) have shown that most of the trigeminal neurons express TrkC in some developmental stages, which is revealed by the careful analyses with Ntrk3$^{tm(Cre)LFR}$ mice. This dynamic change of expression is well correlated with the expression pattern of *HS3ST-2* (Fig 1). Thus, TrkC signaling might be responsible for the regulation of *HS3ST-2* and the target-derived retrograde factor from whisker follicles may be NT-3, a ligand for TrkC receptor.

HS3ST-2/TrkC-expressing neurons define a subset of cutaneous low threshold mechanosensory and muscle-spindle/Golgi tendon proprioceptive/mechanosensory neurons

Although many molecular markers have been identified that sub-classify nociceptive neurons into many specific types, much less is known about mechanosensory neurons. In the TG, previous studies using *TrkC*-null mice revealed that the Merkel cell-associated endings are largely absent in the whisker follicular sinus complexes in these mice, but all other nerve endings are present or observed more frequently (Fundin et al., 1997). This data suggested that Merkel sensory endings may be formed by TrkC-expressing TG neurons. Our results here definitively showed that Merkel endings originate from *TrkC*- and *HS3ST-2*-positive neurons. In addition, longitudinal lanceolate endings also originate from *TrkC*- and *HS3ST-2*-positive neurons and do not express *TrkA* and *TrkB*. It is unclear why only the Merkel endings are affected in *TrkC* mutant mice (Fundin et al., 1997). It could be that the TrkA/B receptors are ectopically expressed in these neurons to compensate for TrkC in TrkC mutant, a possibility that has not been tested. Alternatively, consider that Merkel endings are formed during embryonic stages while lanceolate endings are formed postnatally, TrkC may be only important for the survival of early differentiated Merkel

endings. Our results also showed the spiny endings and a kind of circumferential circular endings, which is presumably transverse lanceolate endings, are weakly positive for *HS3ST-2*, suggesting that different types of nerve endings exhibit different expression levels of *HS3ST-2*. Thus the expression levels of *HS3ST-2* could be used to categorize the cutaneous mechanosensory neurons.

The commonly known proprioceptive endings (muscle spindles or Golgi tendon organs) are strongly labeled by hPLAP activity in HS3ST-2-hPLAP mice. This result is completely consistent with the previous results showing TrkC is primarily expressed in these DRG neurons (Mu et al., 1993; Ernfors et al., 1994; Klein, 1994). It is worth noting that masseter muscle spindle endings formed by trigeminal mesencephalic neurons are also *TrkC* positive, but their survival is not dependent on TrkC signaling (Tessarollo et al., 1994; Kucera et al., 1998; Matsuo et al., 2000). These muscles innervations are weakly positive for HS3ST2-PLAP (data not shown). In addition, we found that *HS3ST-2* is weakly expressed in neurons forming the Merkel endings in the glabrous skin of the paws (Fig 9), consistent with previous studies (Funfschilling et al., 2004; Krimm et al., 2006). Our two-color *in situ* results showed that *HS3ST-2* is also expressed in a rare population of cRet-positive neurons. Since we found that HS3ST-2-PLAP also weakly stained the transverse lanceolate endings in hairy skin, perhaps these endings originate from cRet-positive neurons, although further studies are needed to have a clear conclusion.

Taken together, TrkC and strong*HS3ST-2* expressions are shared among the muscle innervating sensory neurons which are commonly regarded as proprioceptors or interoceptors, and the Merkel and longitudinal lanceolate ending type of mechanosensory neurons which are normally considered as exteroceptors. Interestingly, Merkel endings of the feet do detect the pressure in contact with the ground, and that both the lanceolate and Merkel endings may contribute to sense the location of the whiskers. Under these circumstance, lanceolate and Merkel endings serve as proprioceptors for feet and whiskers. Thus, we speculate HS3ST-2 might be a common marker associated with sensory neurons that have proprioceptive functions. Consistent with this idea and notably, almost all neurons in the vestibular ganglia are positive for *HS3ST-2*, whereas neurons in the cochlear ganglia do not express *HS3ST-2* at all (Fig 1). Vestibular neurons sense the position or movement of the head and thus can be also viewed as one type of proprioceptive neurons.

Physiological functions of HS3ST-2

Specific O-sulfation of HSPGs has been reported to have important roles in the development of nervous system. The mice deficient in *HS2ST* have a reduced size of cerebral cortex (McLaughlin et al., 2003). Furthermore, *HS2ST* and *HS6ST-1*knock-out mice show severe defects in the axon guidance of retinal ganglion cells (Pratt et al., 2006). In contrast, our homozygous HS3ST-2-PLAP mice were viable and did not show any gross abnormality in their morphology and behavior (data not shown). The AP-staining of embryonic and adult mice sections also did not reveal any abnormality in the nerve pathfinding processes (data not shown). HS3STs are consisted of 6 subtypes of enzymes and a previous study revealed that these subtypes have a different preference in their substrate (Liu et al., 1999; Shworak et al., 1999; Chen et al., 2003; Xu et al., 2005), supporting the possible existence of specific physiological importance. However, the substrate specificity is not strict and they might be able to compensate the function of each subtype (Chen et al., 2003). Considering these facts, we suppose that other family member of HS3STs can substitute the physiological functions of HS3ST-2 in our homozygous mice.

Acknowledgments

We thank Drs. Wenqin Luo and David Ginty for the protocol for two-color *in situ* analysis. We also thank Sara Abbott and Bao-Xia Han for their excellent technical assistance, Amanda K. Wagner for reading and comment on this manuscript and members from the Wang laboratory for useful discussions. We also want to specially thank the anonymous reviewer for many careful and insightful comments and suggestions that helped us interpret our results correctly, and discuss our results appropriately.

This work was supported by NIDCR (5RO1DE16550), the Alfred A. Sloan Foundation, the Klingenstein Fund, the Whitehall Foundation, and the McKnight Scholar award (all to F.W.) and by fellowships from the Uehara Memorial Foundation and the Japan Society for the Promotion of Science (to H.H.).

Literature Cited

Adly MA, Assaf HA, Nada EA, Soliman M, Hussein M. Human scalp skin and hair follicles express neurotrophin-3 and its high-affinity receptor tyrosine kinase C, and show hair cycle-dependent alterations in expression. Br J Dermatol. 2005; 153:514–520. [PubMed: 16120135]

Barbacid M. The Trk family of neurotrophin receptors. J Neurobiol. 1994; 25:1386–1403. [PubMed: 7852993]

Botchkarev VA, Botchkarev NV, Albers KM, van derVeen C, Lewin GR, Paus R. Neurotrophin-3 involvement in the regulation of hair follicle morphogenesis. J Invest Dermatol. 1998; 111:279–285. [PubMed: 9699730]

Buckingham M, Bajard L, Chang T, Daubas P, Hadchouel J, Meilhac S, Montarras D, Rocancourt D, Relaix F. The formation of skeletal muscle: from somite to limb. J Anat. 2003; 202:59–68. [PubMed: 12587921]

Cadwallader AB, Yost HJ. Combinatorial expression patterns of heparan sulfate sulfotransferases in zebrafish: I. The 3-O-sulfotransferase family. Dev Dyn. 2006; 235:3423–3431. [PubMed: 17075882]

Carroll P, Lewin GR, Koltzenburg M, Toyka KV, Thoenen H. A role for BDNF in mechanosensation. Nat Neurosci. 1998; 1:42–46. [PubMed: 10195107]

Caterina MJ, Schumacher MA, Tominaga M, Rosen TA, Levine JD, Julius D. The capsaicin receptor: a heat-activated ion channel in the pain pathway. Nature. 1997; 389:816–824. [PubMed: 9349813]

Chao T, Pham K, Steward O, Gupta R. Chronic nerve compression injury induces a phenotypic switch of neurons within the dorsal root ganglia. J Comp Neurol. 2008; 506:180–193. [PubMed: 18022951]

Chen CL, Broom DC, Liu Y, de Nooij JC, Li Z, Cen C, Samad OA, Jessell TM, Woolf CJ, Ma Q. Runx1 determines nociceptive sensory neuron phenotype and is required for thermal and neuropathic pain. Neuron. 2006; 49:365–377. [PubMed: 16446141]

Chen J, Duncan MB, Carrick K, Pope RM, Liu J. Biosynthesis of 3-O-sulfated heparan sulfate: unique substrate specificity of heparin sulfate 3-O-sulfotransferase isoform 5. Glycobiology. 2003; 13:785–794. [PubMed: 12907690]

Cronk KM, Wilkinson GA, Grimes R, Wheeler EF, Jhaveri S, Fundin BT, Silos-Santiago I, Tessarollo L, Reichardt LF, Rice FL. Diverse dependencies of developing Merkel innervation on the trkA and both full-length and truncated isoforms of trkC. Development. 2002; 129:3739–3750. [PubMed: 12117822]

Davis BM, Fundin BT, Albers KM, Goodness TP, Cronk KM, Rice FL. Overexpression of nerve growth factor in skin causes preferential increases among innervation to specific sensory targets. J Comp Neurol. 1997; 387:489–506. [PubMed: 9373009]

Dong X, Han S, Zylka MJ, Simon MI, Anderson DJ. A diverse family of GPCRs expressed in specific subsets of nociceptive sensory neurons. Cell. 2001; 106:619–632. [PubMed: 11551509]

Ebara S, Kumamoto K, Matsuura T, Mazurkiewicz JE, Rice FL. Similarities and differences in the innervation of mystacial vibrissal follicle-sinus complexes in the rat and cat: a confocal microscopic study. J Comp Neurol. 2002; 449:103–119. [PubMed: 12115682]

Ernfors P, Lee KF, Kucera J, Jaenisch R. Lack of neurotrophin-3 leads to deficiencies in the peripheral nervous system and loss of limb proprioceptive afferents. Cell. 1994; 77:503–512. [PubMed: 7514502]

Fundin BT, Rice FL, Pfaller K, Arvidsson J. The innervation of the mystacial pad in the adult rat studied by anterograde transport of HRP conjugates. Exp Brain Res. 1994; 99:233–246. [PubMed: 7523174]

Fundin BT, Silos-Santiago I, Ernfors P, Fagan AM, Aldskogius H, DeChiara TM, Phillips HS, Barbacid M, Yancopoulos GD, Rice FL. Differential dependency of cutaneous mechanoreceptors on neurotrophins, trk receptors, and P75 LNGFR. Dev Biol. 1997; 190:94–116. [PubMed: 9331334]

Funfschilling U, Ng YG, Zang K, Miyazaki J, Reichardt LF, Rice FL. TrkC kinase expression in distinct subsets of cutaneous trigeminal innervation and nonneuronal cells. J Comp Neurol. 2004; 480:392–414. [PubMed: 15558783]

Hasegawa H, Abbott S, Han BX, Qi Y, Wang F. Analyzing somatosensory axon projections with the sensory neuron-specific Advillin gene. J Neurosci. 2007; 27:14404–14414. [PubMed: 18160648]

Hodge LK, Klassen MP, Han BX, Yiu G, Hurrell J, Howell A, Rousseau G, Lemaigre F, Tessier-Lavigne M, Wang F. Retrograde BMP signaling regulates trigeminal sensory neuron identities and the formation of precise face maps. Neuron. 2007; 55:572–586. [PubMed: 17698011]

Huang EJ, Reichardt LF. Trk receptors: roles in neuronal signal transduction. Annu Rev Biochem. 2003; 72:609–642. [PubMed: 12676795]

Klein R. Role of neurotrophins in mouse neuronal development. Faseb J. 1994; 8:738–744. [PubMed: 8050673]

Kramer I, Sigrist M, de Nooij JC, Taniuchi I, Jessell TM, Arber S. A role for Runx transcription factor signaling in dorsal root ganglion sensory neuron diversification. Neuron. 2006; 49:379–393. [PubMed: 16446142]

Krimm RF, Davis BM, Noel T, Albers KM. Overexpression of neurotrophin 4 in skin enhances myelinated sensory endings but does not influence sensory neuron number. J Comp Neurol. 2006; 498:455–465. [PubMed: 16937395]

Kucera J, Fan G, Walro J, Copray S, Tessarollo L, Jaenisch R. Neurotrophin-3 and trkC in muscle are non-essential for the development of mouse muscle spindles. Neuroreport. 1998; 9:905–909. [PubMed: 9579688]

Lawrence R, Yabe T, Hajmohammadi S, Rhodes J, McNeely M, Liu J, Lamperti ED, Toselli PA, Lech M, Spear PG, Rosenberg RD, Shworak NW. The principal neuronal gD-type 3-O-sulfotransferases and their products in central and peripheral nervous system tissues. Matrix Biol. 2007; 26:442–455. [PubMed: 17482450]

Lee JS, Chien CB. When sugars guide axons: insights from heparin sulphate proteoglycan mutants. Nat Rev Genet. 2004; 5:923–935. [PubMed: 15573124]

Leighton PA, Mitchell KJ, Goodrich LV, Lu X, Pinson K, Scherz P, Skarnes WC, Tessier-Lavigne M. Defining brain wiring patterns and mechanisms through gene trapping in mice. Nature. 2001; 410:174–179. [PubMed: 11242070]

Lin X. Functions of heparan sulfate proteoglycans in cell signaling during development. Development. 2004; 131:6009–6021. [PubMed: 15563523]

Liu J, Shworak NW, Sinay P, Schwartz JJ, Zhang L, Fritze LM, Rosenberg RD. Expression of heparan sulfate D-glucosaminyl 3-O-sulfotransferase isoforms reveals novel substrate specificities. J Biol Chem. 1999; 274:5185–5192. [PubMed: 9988768]

Luo W, Wickramasinghe SR, Savitt JM, Griffin JW, Dawson TM, Ginty DD. A hierarchical NGF signaling cascade controls Ret-dependent and Ret-independent events during development of nonpeptidergic DRG neurons. Neuron. 2007; 54:739–754. [PubMed: 17553423]

Matsuo S, Ichikawa H, Silos-Santiago I, Arends JJ, Henderson TA, Kiyomiya K, Kurebe M, Jacquin MF. Proprioceptive afferents survive in the masseter muscle of trkC knockout mice. Neuroscience. 2000; 95:209–216. [PubMed: 10619477]

McKemy DD, Neuhausser WM, Julius D. Identification of a cold receptor reveals a general role for TRP channels in thermosensation. Nature. 2002; 416:52–58. [PubMed: 11882888]

McLaughlin D, Karlsson F, Tian N, Pratt T, Bullock SL, Wilson VA, Price DJ, Mason JO. Specific modification of heparin sulphate is required for normal cerebral cortical development. Mech Dev. 2003; 120:1481–1488. [PubMed: 14654220]

Molliver DC, Radeke MJ, Feinstein SC, Snider WD. Presence or absence of TrkA protein distinguishes subsets of small sensory neurons with unique cytochemical characteristics and dorsal horn projections. J Comp Neurol. 1995; 361:404–416. [PubMed: 8550888]

Molliver DC, Wright DE, Leitner ML, Parsadanian AS, Doster K, Wen D, Yan Q, Snider WD. IB4-binding DRG neurons switch from NGF to GDNF dependence in early postnatal life. Neuron. 1997; 19:849–861. [PubMed: 9354331]

Mu X, Silos-Santiago I, Carroll SL, Snider WD. Neurotrophin receptor genes are expressed in distinct patterns in developing dorsal root ganglia. J Neurosci. 1993; 13:4029–4041. [PubMed: 8366358]

Peier AM, Moqrich A, Hergarden AC, Reeve AJ, Andersson DA, Story GM, Earley TJ, Dragoni I, McIntyre P, Bevan S, Patapoutian A. A TRP channel that senses cold stimuli and menthol. Cell. 2002; 108:705–715. [PubMed: 11893340]

Peters EM, Botchkarev VA, Muller-Rover S, Moll I, Rice FL, Paus R. Developmental timing of hair follicle and dorsal skin innervation in mice. J Comp Neurol. 2002; 448:28–52. [PubMed: 12012374]

Pratt T, Conway CD, Tian NM, Price DJ, Mason JO. Heparan sulphation patterns generated by specific heparin sulfotransferase enzymes direct distinct aspects of retinal axon guidance at the optic chiasm. J Neurosci. 2006; 26:6911–6923. [PubMed: 16807321]

Priestley JV, Michael GJ, Averill S, Liu M, Willmott N. Regulation of nociceptive neurons by nerve growth factor and glial cell line derived neurotrophic factor. Can J Physiol Pharmacol. 2002; 80:495–505. [PubMed: 12056559]

Rice FL, Albers KM, Davis BM, Silos-Santiago I, Wilkinson GA, LeMaster AM, Ernfors P, Smeyne RJ, Aldskogius H, Phillips HS, Barbacid M, DeChiara TM, Yancopoulos GD, Dunne CE, Fundin BT. Differential dependency of unmyelinated and A delta epidermal and upper dermal innervation on neurotrophins, trk receptors, and p75LNGFR. Dev Biol. 1998; 198:57–81. [PubMed: 9640332]

Rice FL, Fundin BT, Arvidsson J, Aldskogius H, Johansson O. Comprehensive immunofluorescence and lectin binding analysis of vibrissal follicle sinus complex innervation in the mystacial pad of the rat. J Comp Neurol. 1997; 385:149–184. [PubMed: 9268122]

Rice FL, Kinnman E, Aldskogius H, Johansson O, Arvidsson J. The innervation of the mystacial pad of the rat as revealed by PGP 9.5 immunofluorescence. J Comp Neurol. 1993; 337:366–385. [PubMed: 8282848]

Shah NM, Pisapia DJ, Maniatis S, Mendelsohn MM, Nemes A, Axel R. Visualizing sexual dimorphism in the brain. Neuron. 2004; 43:313–319. [PubMed: 15294140]

Shworak NW, Liu J, Petros LM, Zhang L, Kobayashi M, Copeland NG, Jenkins NA, Rosenberg RD. Multiple isoforms of heparan sulfate D-glucosaminyl 3-O-sulfotransferase. Isolation, characterization, and expression of human cdnas and identification of distinct genomic loci. J Biol Chem. 1999; 274:5170–5184. [PubMed: 9988767]

Snider WD. Functions of the neurotrophins during nervous system development: what the knockouts are teaching us. Cell. 1994; 77:627–638. [PubMed: 8205613]

Snider WD, McMahon SB. Tackling pain at the source: new ideas about nociceptors. Neuron. 1998; 20:629–632. [PubMed: 9581756]

Story GM, Peier AM, Reeve AJ, Eid SR, Mosbacher J, Hricik TR, Earley TJ, Hergarden AC, Andersson DA, Hwang SW, McIntyre P, Jegla T, Bevan S, Patapoutian A. ANKTM1, a TRP-like channel expressed in nociceptive neurons, is activated by cold temperatures. Cell. 2003; 112:819–829. [PubMed: 12654248]

Tessarollo L, Vogel KS, Palko ME, Reid SW, Parada LF. Targeted mutation in the neurotrophin-3 gene results in loss of muscle sensory neurons. Proc Natl Acad Sci U S A. 1994; 91:11844–11848. [PubMed: 7991545]

Torsney C, Anderson RL, Ryce-Paul KA, MacDermott AB. Characterization of sensory neuron subpopulations selectively expressing green fluorescent protein in phosphodiesterase 1C BAC transgenic mice. Mol Pain. 2006; 2:17. [PubMed: 16681857]

Wilson PO, Barber PC, Hamid QA, Power BF, Dhillon AP, Rode J, Day IN, Thompson RJ, Polak JM. The immunolocalization of protein gene product 9.5 using rabbit polyclonal and mouse monoclonal antibodies. Br J Exp Pathol. 1988; 69:91–104. [PubMed: 2964855]

Xia G, Chen J, Tiwari V, Ju W, Li JP, Malmstrom A, Shukla D, Liu J. Heparan sulfate 3-O-sulfotransferase isoform 5 generates both an antithrombin-binding site and an entry receptor for herpes simplex virus, type 1. J Biol Chem. 2002; 277:37912–37919. [PubMed: 12138164]

Xu D, Tiwari V, Xia G, Clement C, Shukla D, Liu J. Characterization of heparin sulphate 3-O-sulphotransferase isoform 6 and its role in assisting the entry of herpes simplex virus type 1. Biochem J. 2005; 385:451–459. [PubMed: 15303968]

Yabe T, Hata T, He J, Maeda N. Developmental and regional expression of heparan sulfate sulfotransferase genes in the mouse brain. Glycobiology. 2005; 15:982–993. [PubMed: 15944372]

Yoshikawa M, Senzaki K, Yokomizo T, Takahashi S, Ozaki S, Shiga T. Runx1 selectively regulates cell fate specification and axonal projections of dorsal root ganglion neurons. Dev Biol. 2007; 303:663–674. [PubMed: 17208218]

Zylka MJ, Dong X, Southwell AL, Anderson DJ. Atypical expansion in mice of the sensory neuron-specific Mrg G protein-coupled receptor family. Proc Natl Acad Sci U S A. 2003; 100:10043–10048. [PubMed: 12909716]

Zylka MJ, Rice FL, Anderson DJ. Topographically distinct epidermal nociceptive circuits revealed by axonal tracers targeted to Mrgprd. Neuron. 2005; 45:17–25. [PubMed: 15629699]

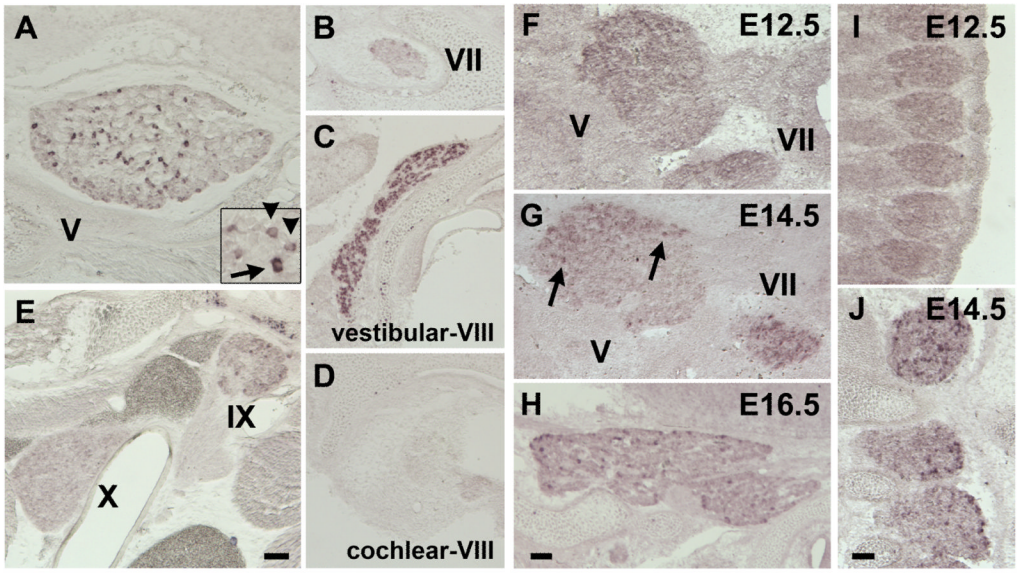

Figure 1.

HS3ST-2 mRNA expression in the developing sensory ganglia. **A**–**E:** Coronal sections of P0 neonatal head were hybridized with *HS3ST-2*cRNA probe. **A:** *HS3ST-2* was detected in a subset of trigeminal neurons. The intensity of the signal was different in each cell (inset, arrow and arrowheads). **B**–**E:** *HS3ST-2* was detected in a subset of neurons in the facial (VII) ganglia (B) and glossopharyngeal (IX) ganglia (E). Almost all neurons expressed *HS3ST-2* in the vestibular (a part of VIII) ganglia (C), whereas no cells were positive for *HS3ST-2* in the cochlear (another part of VIII) ganglia (D). A very few neurons were positive in the vagus (X) ganglia (E). **F**–**J:** Transverse sections of E12.5 (F), E14.5 (G) and E16.5 (H) TG and E12.5 (I) and E14.5 (J) DRG. *HS3ST-2* was detected most of the cells in the ophthalmic and maxillary divisions at E12.5 (F). Subpopulation of the cells began to express *HS3ST-2* at E14.5 (G, arrows) and the expression level increased during development (H and A). In contrast, no signal was observed by E12.5 in the DRG (I). A subset of the neurons began to express *HS3ST-2* at E14.5 (J). Scale bars, 100 μm.

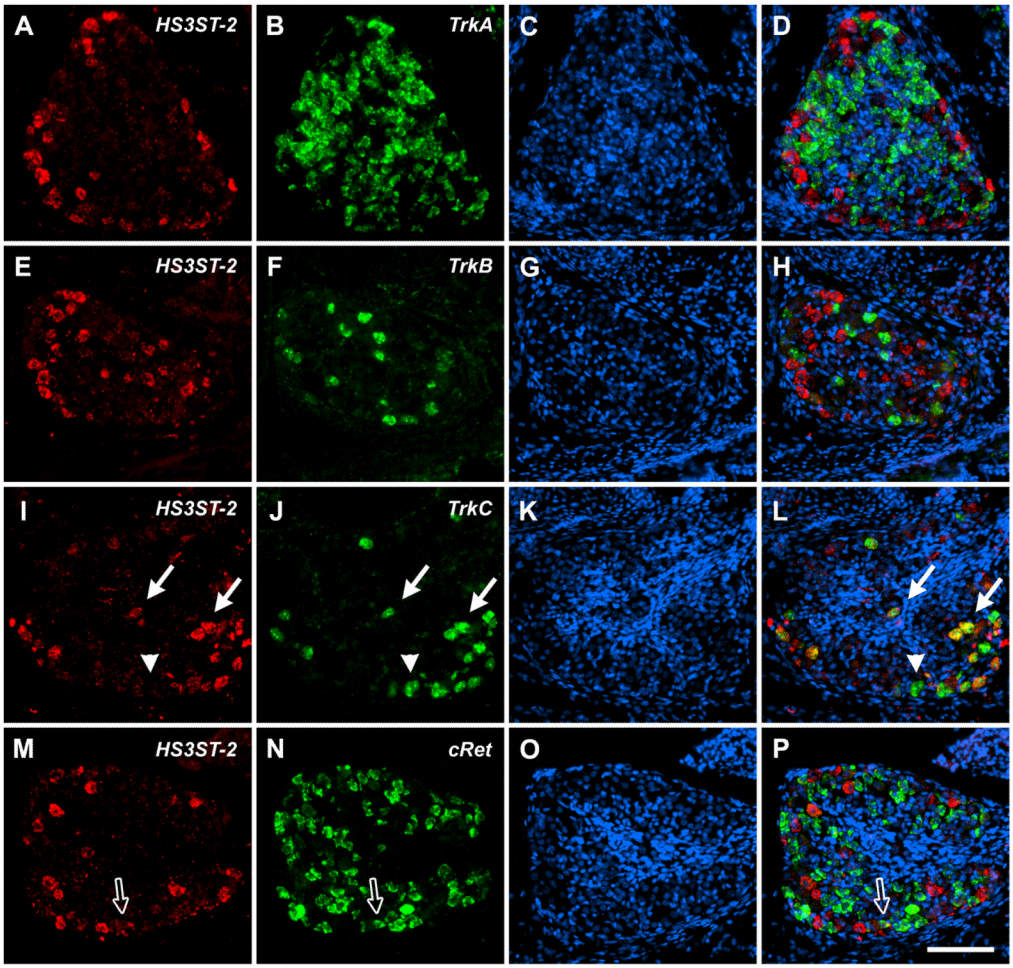

Figure 2.

Co-localization of *HS3ST-2* mRNA with receptors for neurotrophic factors in the DRG. P0 neonatal DRG coronal sections were hybridized with the cRNA probes for *TrkA*, *TrkB*, *TrkC* or *cRet* combined with *HS3ST-2*. *HS3ST-2* did not co-localize with *TrkA* or *TrkB*. Most of the *HS3ST-2* signal was also positive for *TrkC* (arrows), although some of the *TrkC*-positive cells did not express *HS3ST-2* (arrowhead). The majority of the *cRet*-positive cells were negative for *HS3ST-2*, but a very few cells were found to express both *cRet* and *HS3ST-2* (open arrow). Scale bar, 100 μm.

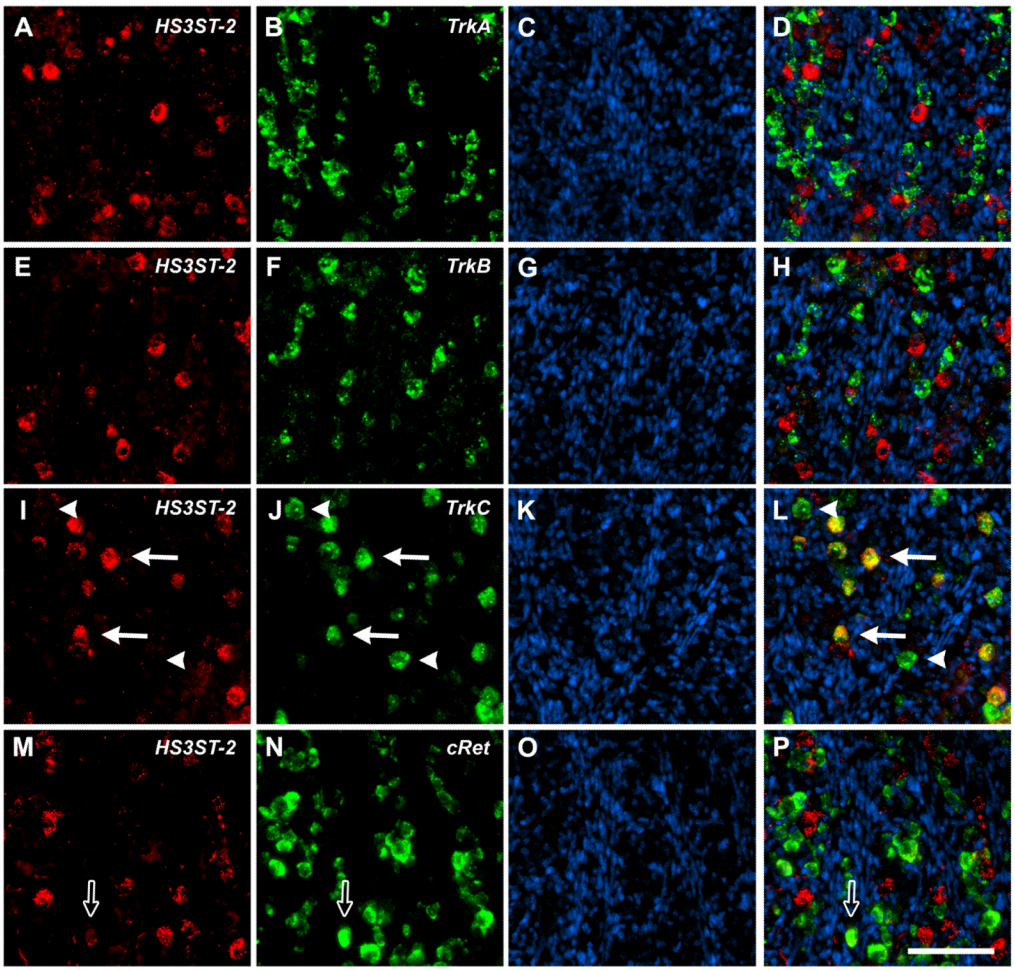

Figure 3.

Co-localization of *HS3ST-2* mRNA with receptors for neurotrophic factors in the TG. P0 neonatal TG coronal sections were hybridized with the cRNA probes for *TrkA*, *TrkB*, *TrkC* or *cRet* combined with *HS3ST-2*. Similarly to the results in DRG sections, *HS3ST-2* did not co-localized with *TrkA* or *TrkB*. The *HS3ST-2* signal was almost completely co-localized with *TrkC* (arrows), although a few *TrkC*-positive cells did not express *HS3ST-2* (arrowheads). Most of the *cRet*-positive cells were negative for *HS3ST-2*, but only a very few cells were positive for *HS3ST-2* (open arrow). Scale bar, 100 μm.

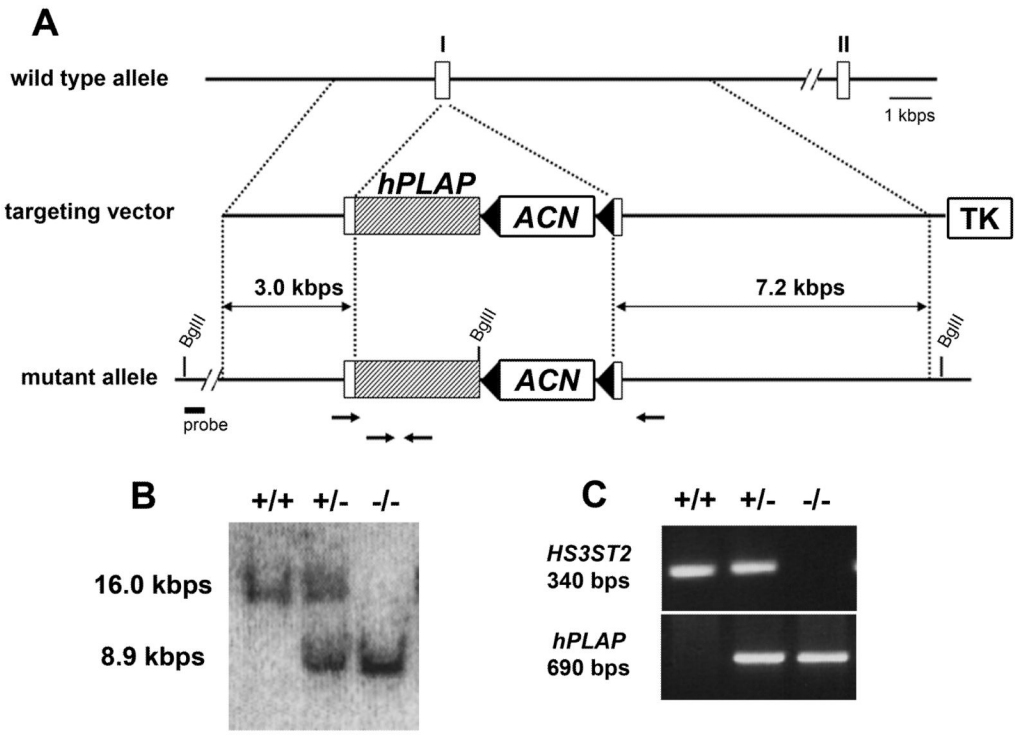

Figure 4.

Targeted insertion of the *hPLAP* gene into the *HS3ST-2* locus. **A:** Schematic representation of the gene insertion. The *hPLAP* gene with an *ACN* cassette was inserted at the translational start codon of the *HS3ST-2* gene. Exons are represented as white boxes. The thymidine kinase cassette is designated as TK. Arrows indicate the position of primers used for genomic PCR analysis. **B:** Southern blot analysis of genomic DNA from wild type, heterozygous and homozygous mice. The 16.0 and 8.9 kb BglII restriction fragments indicate wild type and mutant alleles, respectively. **C:** Genomic PCR analysis of the progeny. Wild type and mutant alleles produce 340 and 690 bp fragments, respectively.

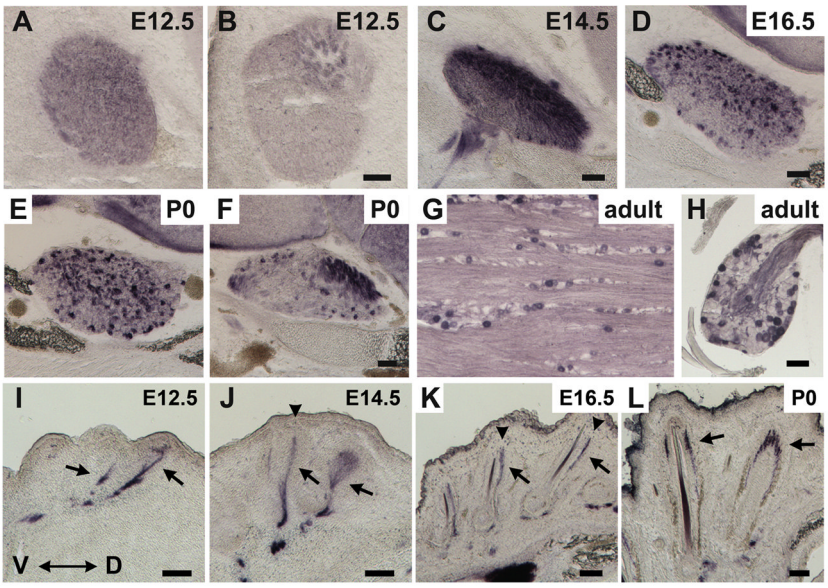

Figure 5.

HS3ST-2-positive neurons visualized by AP-staining in HS3ST-2-hPLAP mice. **A–F:** the hPLAP expression in the developing TG. The expression of hPLAP began by E12.5, when it was found only in the rostral regions (A) but not in the caudal region (B). The intensity increased by E14.5 with the expression in almost all cells and a subset of the cells began to expressing hPLAP strongly by E16.5, when other cells lost the expression (C and D). This was more obvious at P0. The caudal region also has a subset of cells strongly express hPLAP, although the number of the cells was smaller than in the rostral regions (E and F). **G:** Transverse section of adult TG. **H:** Coronal section of adult DRG. hPLAP activity was observed strongly in some cells and weakly in other cells. **I–L:** sequential development of whisker-innervating *HS3ST-2*-positive nerve endings. Coronal sections of developing mystacial pads were stained by hPLAP activity. At E12.5 (I) and E14.5 (J), most axons were found at the developing FSC and form a plexus, which are presumptive DVN axons (arrows). At E16.5, Merkel endings at the ring sinus level started to form (K). Both at E14.5 and E16.5, the dorsal projections were more intensely positive than the ventral projections (J and K, arrowheads). At P0, Merkel endings and longitudinal lanceolate endings, but not other type of endings, are observed (L, arrows). Dorsal is right and ventral is left. Scale bars, 100 μm.

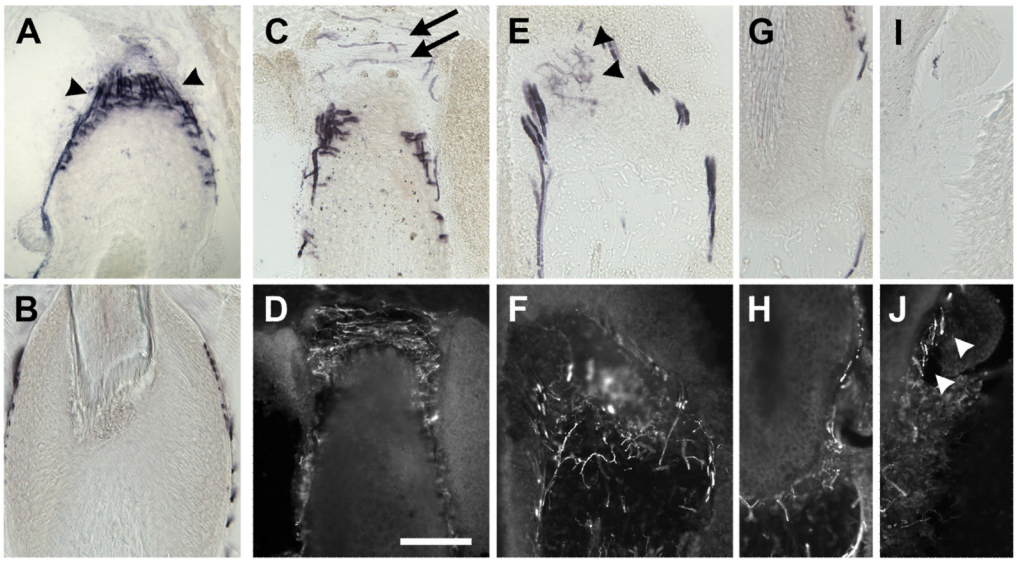

Figure 6.
Diverse sensory endings in the FSC visualized by AP-staining in HS3ST-2-hPLAP mice. Transverse sections of adult mystacial pads were first stained with AP activity (A, B, C, E, G, I), and then co-stained with the antibody against PGP9.5 (D, F, H, J). The longitudinal lanceolate endings (A, arrowheads) and Merkel endings (B) were intensely positive for the hPLAP activity. A type of circumferential circular endings (C and D, arrows, probably transverse lanceolate endings) and rare spiny endings (E, arrowheads) were found to be weakly positive, whereas many of these endings were negative. None of the reticular endings (G and H) and club-like endings (I and J, arrowheads) was stained by hPLAP activity. Scale bar, 100 μm.

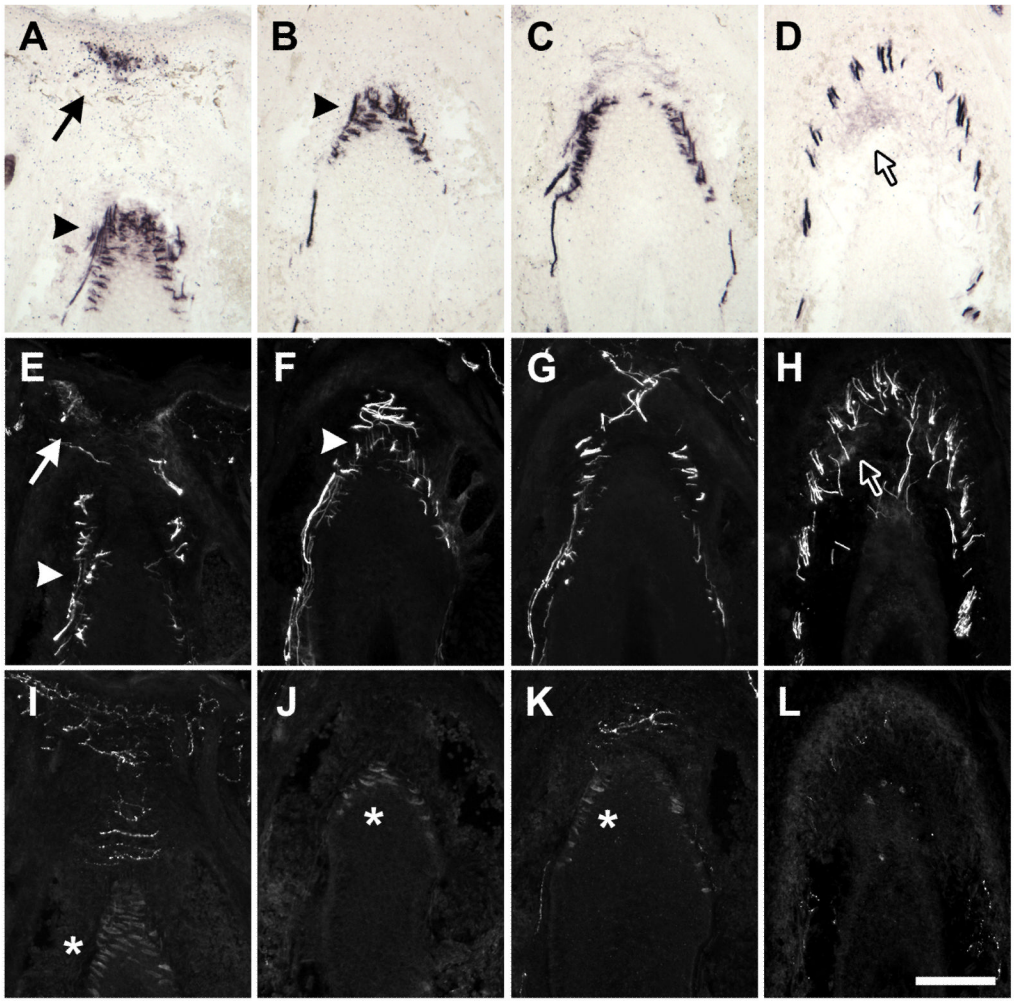

Figure 7.

Further characterization of HS3ST-2-hPLAP positive sensory endings. The serial sections from HS3ST-2-hPLAP mystacial pads were stained by AP-activity (A–D) or with anti-NF200 (E–H) or anti-CGRP antibody (I–L). The Merkel endings at the rete ridge collar were strongly positive for hPLAP (A, arrow). This type of ending was also positive for NF200 (E). The NF200-positive and CGRP-negative longitudinal lanceolate endings were strongly stained for hPLAP (A, B, E, F, I and J, arrowheads). A small population of circumferential circular endings was weakly detected by hPLAP activity but their reactivity to NF200 and CGRP are not conclusive (C, G and K). Some of spiny endings, which are NF200-positive and CGRP-negative, are also labeled by hPLAP (D, H and L, open arrows). Note that Merkel cells themselves are CGRP-positive (asterisks). Scale bar; 100 μm.

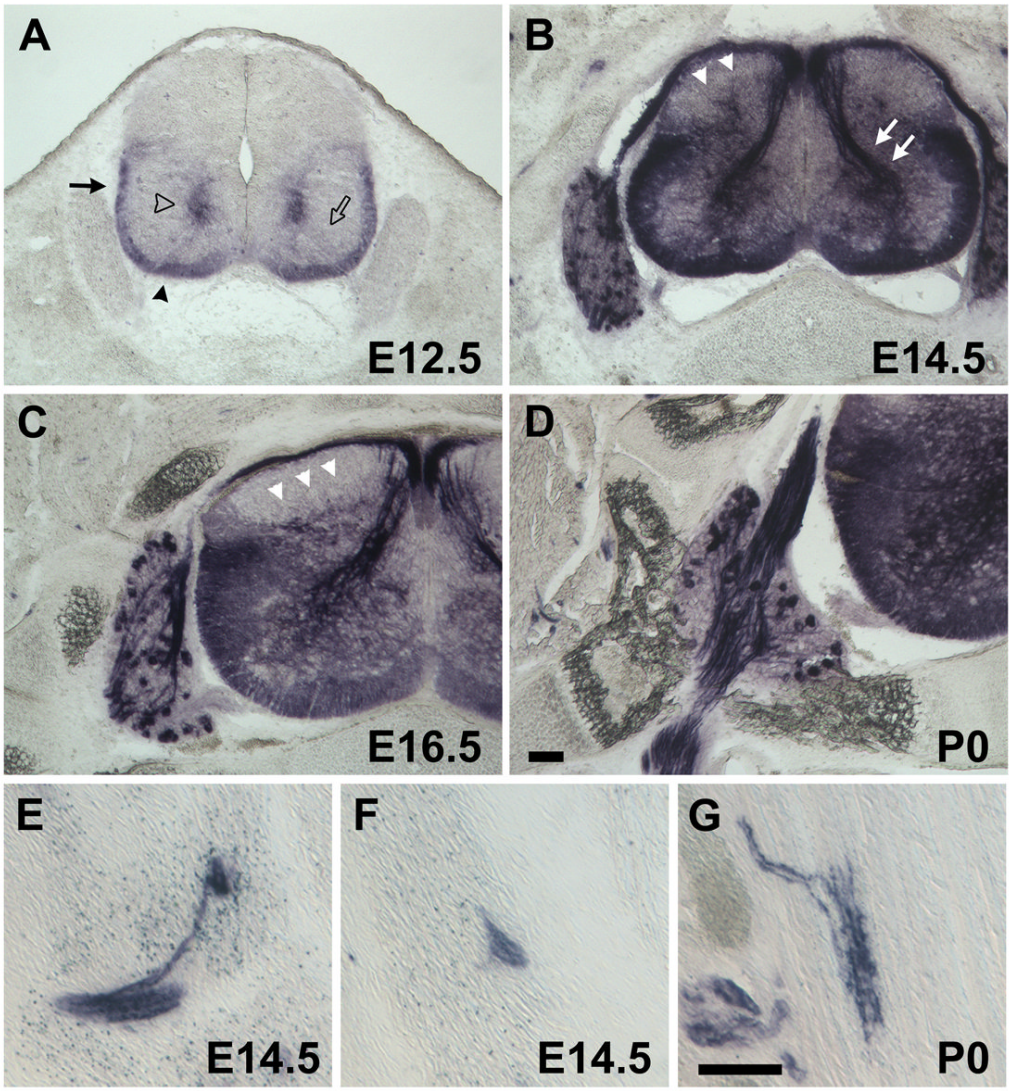

Figure 8.

Developmental expression of hPLAP in the DRG of HS3ST-2-hPLAP mice. **A**–**D:** Coronal sections of the developing HS3ST-2-hPLAP embryonic body were stained by hPLAP activity. No signal was observed in the DRG at E12.5, although the motor columns (A, open arrowhead), the spinocerebellar tract (A, arrow) and the vestibulospinal tract (A, arrowhead) were positive for hPLAP activity. The ventral motor roots were weakly stained (A, open arrow). The punctuate expression of hPLAP started at E14.5 and continued throughout development (B–D). The central proprioceptive afferents were clearly stained as early as E14.5 (B, arrows). Weakly stained axons innervate the layer III/IV (B and C, arrowheads). **E**–**G:** Development of the proprioceptive nerve endings. The differentiating immature endings affiliated with developing muscles and tendons could be found at E14.5 (E and F). The nerve endings develop throughout development and are completely differentiated by birth (G). Scale bars, 100μm.

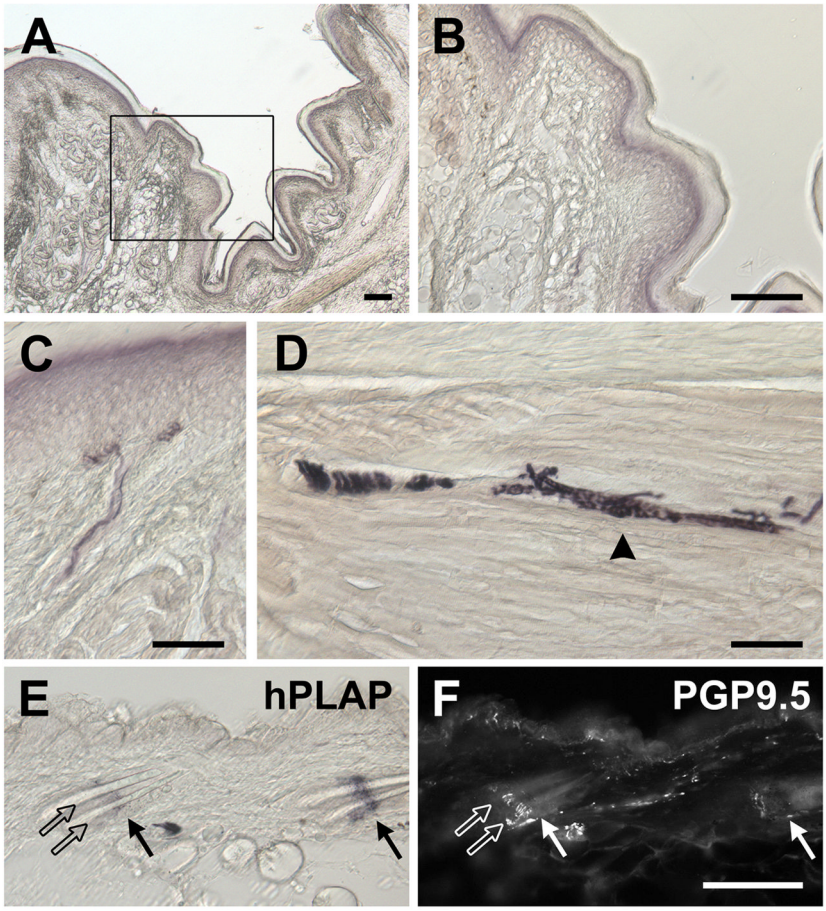

Figure 9.

Peripheral nerve endings visualized by AP-staining in HS3ST-2-hPLAP mice. **A–C:** The sections of the forelimb footpads were developed by the AP-staining. Most of the nerve endings were not stained (A and B), whereas only a few Merkel endings were weakly positive for hPLAP (C). **D:** The muscle spindles (arrowhead) in the skeletal muscles on the same sections were strongly stained. **E and F:** In the hairy skin, the transverse lanceolate endings were specifically labeled (arrows), although longitudinal lanceolate endings and Merkel endings were negative (open arrows). Scale bars, 100 μm.